Two quantum dot systems in lateral arrangement with strong electrostatic interaction: Tool for studying Kondo correlations in electrical transport

J. Weis, A. Hübel, K. Held and K. v. Klitzing

Electrons confined in a quantum dot possess a discrete single-particle energy spectrum. Due to this property, quantum dots are also denoted as 'artificial atoms'. Weakly coupled by tunnel barriers to a source and a drain lead, electrical transport through a quantum dot is dominated by the repulsive electron-electron interaction on the quantum dot site. Such a quantum dot system behaves as a single-electron transistor: By increasing the voltage applied to an adjacent gate electrode, the electron number on the quantum dot site is increased one by one, i.e., under a small source-drain bias voltage, the electrical conductance is repeatedly modulated between single-electron tunneling and Coulomb blockade regime ('Coulomb blockade oscillations').

In 1998, it was experimentally proven that, under certain conditions, such a quantum dot system shows Kondo physics [1] as it was already predicted in 1988 by mapping a single quantum dot system on the Anderson impurity model [2]: The presence of a spin-degeneracy on the quantum dot site induces at low temperature correlated electron tunneling between the quantum dot and the leads, forming overall a spin-singlet state. A highly conductive channel of transport is opened between the leads via the quantum dot, which even reaches the conductance $2e^2/h$ in the case of symmetric tunnel couplings to the leads – the value also found for a spin-degenerate one-dimensional channel. Increasing the temperature breaks the correlations, the Kondo effect is destroyed, and the Coulomb blockade effect is recovered.

The Anderson impurity model describes a spin-degenerate energy level at an impurity or a quantum dot site which is coupled through tunneling to a Fermi sea containing electrons of both spin orientations. In other words, it describes two separate electron subsystems labeled by a two-valued index which is usually identified with the spin quantum number (Fig. 9(a)). The two spin electron systems interact only on the impurity site through Coulomb interaction which suppresses double occupancies of the impurity.

In 2001, we pointed out that two electrostatically coupled quantum dots with separate leads (Fig. 9(b)) reflect a pseudo-spin representation of the Anderson impurity model [3]: This mapping is valid if (1) the quantum dot systems are energetically degenerated, i.e., occupying either dot costs the same energy, (2) the ground state of each quantum dot is not degenerate and excited states are energetically well separated. In case of a spin degeneracy in one or both quantum dot systems, spin and electrostatic (orbital) Kondo effect interplay.

Where do we expect to see these Kondo correlations? Two quantum dot systems with electrostatic interaction have a characteristic honeycomb-like charge stability diagram as a function of two gate voltages that shift the electrostatic potential of the quantum dots differently (see Fig. 9(c)).

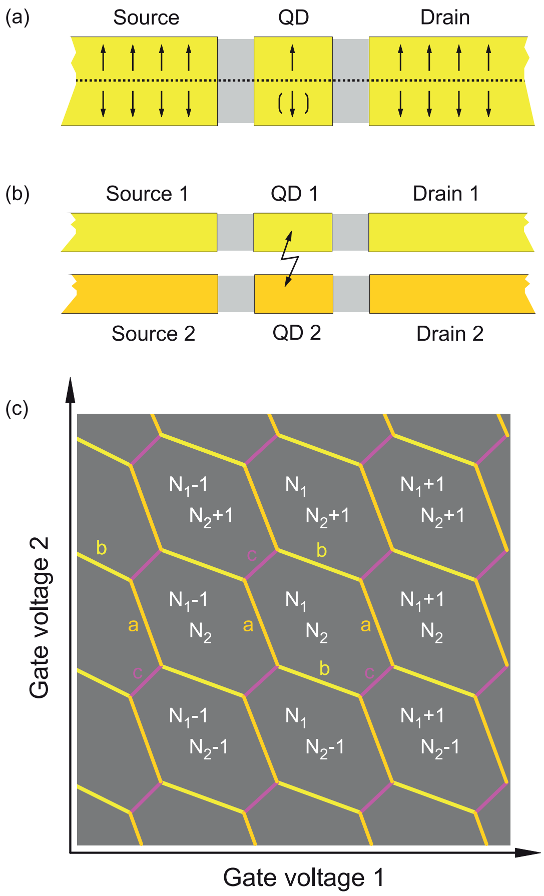

Figure 9: Possible realizations of the Anderson impurity model: (a) Single quantum dot system with spin-degeneracy, or (b) two electrostatically coupled quantum dot systems without spin-degeneracy. (c) Charge stability diagram vs. two gate voltages for arrangement (b). N_1 and N_2 denotes the number of electrons in the respective dot.

Along borderlines, labeled by **a** and **b**, where the electron number in one quantum dot changes by one whereas the electron number in the other remains unchanged, single-electron tunneling through the respective quantum dot is possible. Along borderlines, labeled by **c**, where the electron number in one dot is increased while in the other dot decreased, single-electron tunneling is not possible. However correlated electron tunneling is allowed switching between the two adjacent charge configurations.

Such borderlines **c** are only present if electrostatic interaction between the dots exists, otherwise the triple points at the ends of the borderline **c** merge. The borderlines **c** become longer with stronger interaction. Here we state the existence of a Kondo correlated state at low temperature leading to high conductance through both quantum dots.

To prove the presence of Kondo correlations in two electrostatically coupled quantum dot systems, we have investigated extensively two vertically stacked quantum dot systems realized in a $GaAs/Al_xGa_{1-x}As$ heterostructure ($x = 0.33$) containing two quantum wells with a two-dimensional electron system (2DES) in each well, separated by an insulating 40 nm thick $Al_xGa_{1-x}As$ barrier [4]. We obtained an interdot capacitance of about half the total capacitance C_Σ of a single quantum dot, i.e., the interaction energy is half the single-electron charging energy e^2/C_Σ of a single quantum dot. The electrical characterization measurements indeed indicate the existence of the Kondo correlation [4], including the expected logarithmic decay of the conductance on the **c**-line with temperature.

However, in the parameter regime of interest, we lack the independent control of the four tunnel barriers in the structure: One quantum dot was coupled to its source and drain whereas the second was only connected to its source, i.e., the electrical transport through only one quantum dot system was measurable. Therefore, the second dot could not be fully characterized, especially the strength of the tunnel coupling to the remaining lead was unknown.

To overcome the conceptional lack of in situ tunability in our vertically stacked arrangement – three voltage parameters for four tunnel barriers, we have now realized two quantum dot systems with strong capacitive interdot coupling in a *lateral* arrangement in a two-dimensional electron system buried 50 nm below the surface of a $GaAs/Al_{1-x}Ga_xAs$ heterostructure ($x = 0.33$). Strong electrostatic interaction between the dots is not trivially obtained in this geometry. This has been achieved by using a floating metal electrode covering both quantum dots.

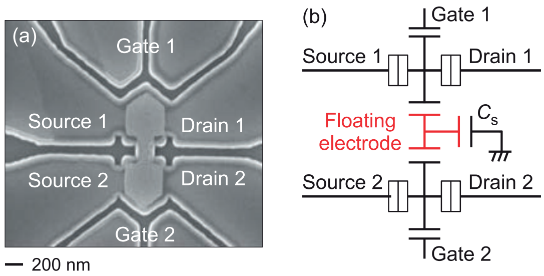

Figure 10: (a) Scanning electron microscope image of the etched heterostructure surface. The two-dimensional electron system is divided into different regions acting as quantum dots, leads and gates. A metal electrodes covers both quantum dot regions. (b) Capacitance circuit describing the arrangement. The stray capacitance C_S of the floating metal electrode has to be diminished.

The technique was already used by another group where the quantum dots were defined by electrostatic depletion via split-gates on the heterostructure surface [5], however with few success. In our approach, we defined our quantum dot systems by etching into the heterostructure, dividing the two-dimensional electron system into regions acting as quantum dots, leads and gates (Fig. 10(a)). In this way we could suppress capacitive coupling of the floating gate to gate electrodes in the surrounding, strengthening the capacitive interdot coupling (Fig. 10(b)). Also the shape of the floating electrode has been optimized to minimize the capacitive coupling to the leads [6]. Finally, in the weak tunnel coupling regime, a ratio of 0.35 between interdot capacitance and total capacitance of a single dot has been achieved in our new structure – less than in the vertically stacked arrangement (up to 0.5), however significant more than in previous lateral arrangements (< 0.2).

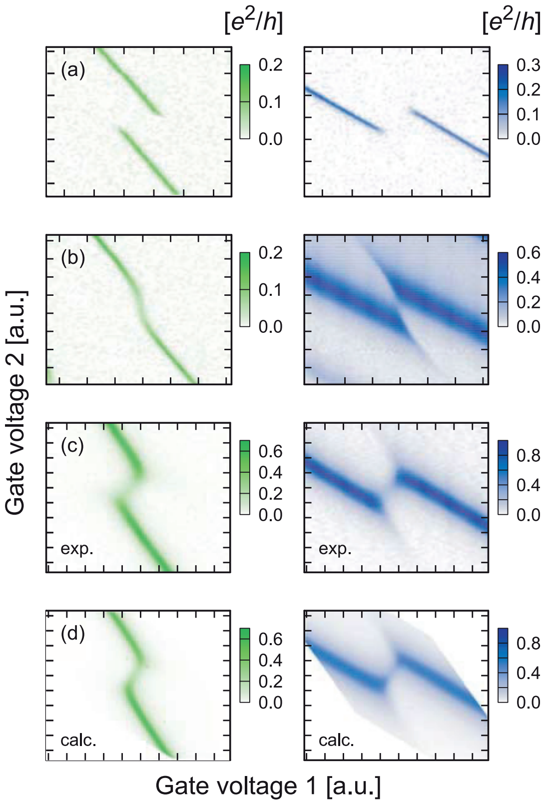

Figure 11: The conductance of quantum dot 1 (left) and 2 (right) as a function of two gate voltages measured around a ***c***-line of the charge stability diagram. From (a) to (b), the tunnel couplings to the leads of quantum dot 2 were increased. Between (a) and (c), the tunnel coupling of both quantum dots were simultaneously enhanced. (d) NRG calculation for case (c).

In Fig. 11 the conductances through the two quantum dots in a region around a **c**-line of the charge stability diagram are shown. The measurements were performed in a ^{3}He–^{4}He dilution refrigerator at base temperature of $T = 25$ mK. From Fig. 11(a) to (b), only the tunnel couplings to the leads of quantum dot 2 were increased, whereas between Fig. 11(a) and (c), the tunnel couplings of both quantum dots were simultaneously enhanced. Striking is that for weak tunnel coupling, no conductance is visible along the **c**-line, whereas with increasing the tunnel coupling, conductance appears.

This is expected since with increasing the tunnel coupling, correlated tunneling is enhanced. However, the position of the conductance peak does not follow exactly the **c**-line extracted from the observed single-electron tunneling peaks in Fig. 11(a). For the situation of different tunnel coupling of both dots (Fig. 11(b)), we could find an analytical expression for describing the position of conductance of quantum dot 1 by simply assuming that the strong tunnel coupled quantum dot 2 is only partially charged with the charge calculated by integrating over the part of a life-time broadened (= Lorentzian-shaped) energy level lying below the Fermi level of the leads. As the weakly tunnel coupled quantum dot 1 switches between well quantized charge states, the broadened energy level of dot 2 is shifted in energy between two values given by the electrostatic interdot coupling and the applied voltages. Having expressions for the total electrostatic energy of both situations, the gate voltage position of electrostatic degeneracy for switching the charge state of quantum dot 1 by an electron charge is found. It fits – except for a small offset – to the position for conductance in quantum dot 1 found in the experiment.

From these considerations for Fig. 11(b), it seems that simple single-electron tunneling happens through quantum dot 1 while charge-polarizing quantum dot 2. However the conductance heights and the temperature dependencies are different in the charge stability diagram at the **a**- and the **c**-line. For same tunnel coupling of both quantum dots (Fig. 11(c)), the picture of above does not hold. In any case, calculating the conductances through the dots is not that simple. This was done by using a numerical renormalization group (NRG) method, allowing for a numerical exact solution of the Anderson impurity model.

Using the parameters extracted from the experimental data in the regime of single electron tunneling of the respective quantum dot and the geometry of the honeycomb pattern, the observed conductance behavior of the electrostatically coupled quantum dot system could nicely be reproduced (an example is shown in Fig. 11(d)).

The comparison yields that the Kondo temperature of the system is below our working temperature, i.e., only the onset of the Kondo correlated state is visible in the experiment. Being limited by the base temperature of a ^{3}He–^{4}He dilution refrigerator, the relevant energies, especially the single-electron charging energies and the interaction energy between the quantum dots have to be enhanced, while keeping the tunability of the tunnel barriers. It requires mainly a reduction of the dot/lead capacitances. Whether underetching of the heterostructure in the tunnel barrier regions helps to improve remains to be clarified.

[1] *Reviewed by L.P. Kouwenhoven and L.I. Glazman.* Revival of the Kondo effect. Physics World, January, 33 (2001).

[2] *Anderson, P.W.* Physical Review **124**, 41–53 (1961).

[3] *Wilhelm, U., J. Schmid, J. Weis and K. v. Klitzing.* Physica E **9**, 625–630 (2001).

[4] *Wilhelm, U., J. Schmid, J. Weis and K. v. Klitzing.* Physica E **14**, 385–390 (2002).

[5] *Chan, I., R. Westervelt, K. Maranowski and A. Gossard.* Applied Physics Letters **80**, 1818–1820 (2002).

[6] *Hübel A., J. Weis, W. Dietsche and K. v. Klitzing.* Applied Physics Letters **91**, 102101 (2007).